Limb Impedance Estimation During Drilling and Screwing Tasks Performed by Human Under Known and Unknown Force Perturbation

HRI-Project-II

Samriddhi Dubey
Mechanical Engineering
24250080

Vidhi Shah
Mechanical Engineering
22110286

I. Introduction

Understanding how humans adapt their limb impedance during physical tasks is essential for advancing Human-Robot Interaction (HRI) research. In this project, we investigate the behavior of human arm impedance when subjected to external perturbations while performing two common manual tasks: **drilling** and **screwing**.

The project focuses on analyzing how a subject maintains tool stability in response to disturbances applied through controlled force perturbations. Two experimental conditions are studied: in the first, the subject does not know the direction of the applied perturbation, and in the second, the subject is aware of it. By capturing position and force data during these tasks, we estimate the dynamic impedance parameters—mass, damping, and stiffness—of the subject's arm.

This study aims to reveal how humans regulate their arm dynamics in different uncertainty scenarios, providing valuable insights for designing more intuitive and adaptive human-robot systems.

II. LITERATURE REVIEW

A. Muscle Synergies and Endpoint Stiffness

Inouye and Valero-Cuevas (2016) present a computational investigation into how experimentally observed muscle synergies constrain the central nervous system's regulation of both endpoint stiffness and energy consumption. Employing a simplified planar arm model with six muscles, they express desired stiffness ellipses and muscle-synergy constraints as linear relationships on activation patterns, and then apply quadratic programming to determine energy-optimal muscle activations. Their analyses demonstrate that the imposition of synergies drastically narrows the repertoire of achievable stiffness orientations and can even preclude energy minimization in certain postures. By reconciling conflicting empirical findings on stiffness modulation, this work reveals posture-dependent trade-offs between mechanical impedance control and metabolic cost, offering insights for both neuromechanical experiments and the design of robotic controllers.

B. Internal Models in Biological Control

McNamee and Wolpert (2019) synthesize a unified account of *internal models*—both forward and inverse—within a probabilistic framework grounded in Bayesian inference and optimal feedback control. They trace the genesis of the internal-model hypothesis from Craik's early cognitive formulations to modern computational theories, detailing how the brain constructs generative models for state estimation, sensory prediction, motor planning, and real-time error correction. This review integrates normative principles to explain a broad spectrum of sensorimotor phenomena, including Bayesian filtering of noisy sensory signals, prospective simulation to overcome neural delays, and feedback control laws that optimize task-relevant costs under uncertainty.

C. Age-Related Alterations in Stiffness Modulation

Gibo *et al.* (2013) examine the effects of healthy aging on the capacity to modulate arm endpoint stiffness in response to directional force perturbations. Using the KINARM exoskeleton, younger (mean 27 years) and older (mean 58 years) adults performed static postural tasks while resisting perturbations along prescribed axes. Although younger participants exhibited selective tuning of both stiffness magnitude and orientation to counter destabilizing forces, older adults showed significantly attenuated stiffness adjustments across conditions. These findings implicate age-related declines in the neural mechanisms underlying optimal impedance regulation, with important implications for the assessment and rehabilitation of motor function in the elderly.

D. Assistive Control via Human Muscular Manipulability

Petrič *et al.* (2019) introduce an exoskeleton control framework that leverages a *muscular manipulability* model to compensate for the inherent anisotropies in human arm force generation. By reshaping the user's anisotropic force manipulability ellipsoid into an isotropic force output across the workspace, the controller provides assistance proportionate to the arm's configuration-dependent weaknesses. In empirical trials with a 2-DoF arm exoskeleton and a 4 kg load task, surface EMG measurements and kinematic analyses confirm

that the proposed method significantly reduces muscular effort without altering natural movement trajectories. This approach demonstrates the efficacy of biomechanically informed manipulability models in designing assistive devices that ensure uniform task performance throughout the reachable workspace.

III. Experimental Design and Setup

A. Subject and Task Design

The human subject's wrist was fixed on a table, which allowed only shoulder and elbow movement. The subject's task was to maintain the tool (drill and screwdriver) on a designated marker attached to the workpiece placed in front of them. The objective was to perform the task accurately despite external disturbances introduced in the system.

B. Perturbation Application

External perturbations were introduced by attaching five strings to the subject's hand. These strings were routed through pulleys, with the free ends hanging off the edge of the table. Known weight of 1 Kg was attached to the free ends of the strings, and this weight was used to generate perturbations. The setup allowed the application of perturbations in various directions and magnitudes during the tasks.

C. Phases of Experiment

1) Unknown Perturbation Phase: In this phase, the subject was unaware of the direction and timing of the applied perturbations. Noise-canceling headphones were used to ensure that there were no auditory cues that could help the subject predict when or where the perturbations would occur. The goal was to test how the subject adapted to random disturbances during the task.

2) Known Perturbation Phase: During this phase, the subject was informed beforehand which string would be perturbed and when. This allowed for a comparison of the subject's response to known disturbances versus unknown disturbances. The objective was to investigate how the subject's adaptive responses varied based on their knowledge of the perturbation.

D. Motion Capture and Force Measurement

The Vicon motion capture system was employed to capture 3D position data with high accuracy. Markers were placed on the human wrist and five additional markers were positioned on the pulleys. Precise tracking of the subject's movements was crucial for analyzing the impact of perturbations on the task performance.

E. Tasks Performed

The subject performed two tasks in this experiment:

1) Drilling Task: In the drilling task as shown in figure 1 , the subject's goal was to keep the drill bit accurately on a designated marker attached to the workpiece. Perturbations were applied during this task to investigate how the subject's arm impedance adjusted to maintain control over the drill during random and known disturbances.

2) Screwing Task: Similarly, in the screwing task as shown in 2, the subject aimed to keep the screwdriver on a designated marker on the workpiece. Again, perturbations were introduced to examine how the subject's limb impedance adapted to the screw-driving motion under external disturbances.

Data Collection and Analysis

F. Data Collection

The Vicon system recorded position, velocity, and acceleration data for the arm and five pulleys for each trial. A total of 21 trials were conducted for both known and unknown perturbations in the case of drilling and screwing, and the data were saved as .csv files.

G. Impedance Estimation

The collected data were analyzed to estimate the subject's dynamic impedance characteristics, including the mass, damping, and stiffness matrices. These matrices are essential for understanding how the subject's limb dynamics change under external perturbations. The estimation was carried out using regression techniques, such as least squares regression, to determine the impedance parameters that best fit the recorded data.

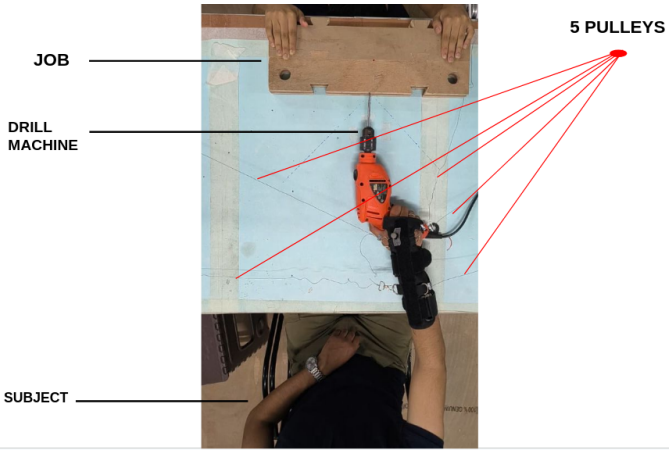

Figure 1: Experimental setup for estimating the limb impedance with known and unknown perturbations while drilling.

IV. MATHEMATICAL MODELLING

A. The 2D Second-Order Dynamic Model

The system is governed by the following second-order differential equation:

$$M\ddot{x} + B\dot{x} + Kx = F,$$

where:

- $x = \begin{bmatrix} x \\ y \end{bmatrix}$ is the 2D position vector.
- $F = \begin{bmatrix} F_x \\ F_y \end{bmatrix}$ is the applied force vector.

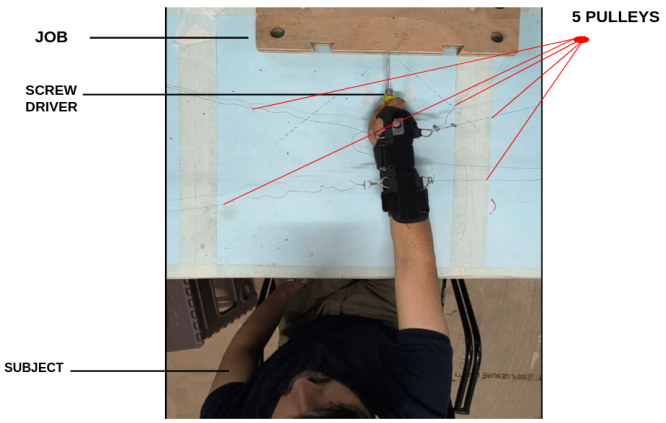

Figure 2: Experimenatl setup for estimating the limb impedance with known and unknown perturbations while screwing.

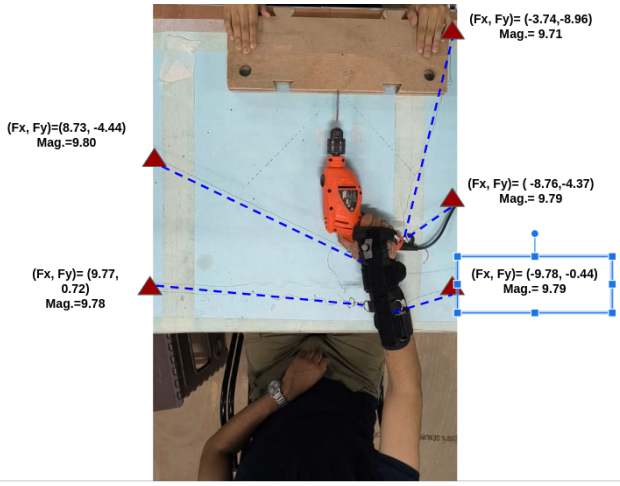

Figure 3: Force vectors applied by different pulleys on the human arm

- M, B, K are the mass, damping, and stiffness matrices, respectively. These matrices are symmetric 2×2 matrices as the system is in 2D.

Thus, the general dynamic equation can be expanded as:

$$\begin{bmatrix} M_{11} & M_{12} \\ M_{12} & M_{22} \end{bmatrix} \begin{bmatrix} \ddot{x} \\ \ddot{y} \end{bmatrix} + \begin{bmatrix} B_{11} & B_{12} \\ B_{12} & B_{22} \end{bmatrix} \begin{bmatrix} \dot{x} \\ \dot{y} \end{bmatrix} + \begin{bmatrix} K_{11} & K_{12} \\ K_{12} & K_{22} \end{bmatrix} \begin{bmatrix} x \\ y \end{bmatrix} = \begin{bmatrix} F_x \\ F_y \end{bmatrix}$$

In this equation:

- M, B, K represent the mass, damping, and stiffness matrices, respectively.
- $\ddot{x}, \ddot{y}$ are the accelerations.
- $\dot{x}, \dot{y}$ are the velocities.
- x, y are the displacements.
- F_x, F_y are the applied forces in the x- and y-directions.

B. Objective: Estimation of M, B, K

The goal is to estimate the unknown coefficients in the matrices M, B, and K. These coefficients are:

$$[M_{11}, M_{12}, M_{22}, B_{11}, B_{12}, B_{22}, K_{11}, K_{12}, K_{22}]$$

Each of these values corresponds to a term in the mass, damping, and stiffness matrices that needs to be estimated based on the experimental data.

C. Force Component Vectors: Pulley Forces

We consider a system of pulleys where forces are applied. The total system involves 5 pulleys, each of which has two force components: F_x and F_y (forces along the x- and y-directions).

For each pulley, we assume that the applied forces F_x and F_y are known. Thus, for each pulley, we have a pair of forces (F_{x1}, F_{y1}), (F_{x2}, F_{y2}), ..., (F_{x5}, F_{y5}). These force vectors are part of the force vector F in the equation. The force vectors applied bu differnet pulleys on the human arm as shown in figure 3 were found with the help of Vicon data.

In total, for 5 pulleys, the force vector F will be:

$$F = \begin{bmatrix} F_{x1} \\ F_{y1} \\ F_{x2} \\ F_{y2} \\ \vdots \\ F_{x5} \\ F_{y5} \end{bmatrix}$$

We are given the measurements for position (X_i, Y_i), velocity $(\dot{X}_i, \dot{Y}_i)$, and acceleration $(\ddot{X}_i, \ddot{Y}_i)$ for each of the 5 pulleys. These measurements are taken at specific time steps, and they provide the data needed to solve the system of equations.

Each measurement point yields two rows in the matrix A because we are solving for 2 unknowns (one for the x-direction and one for the y-direction) at each point.

For each pulley, the matrix A is built as:

$$A_{2i-1,:} = \left[\ddot{X}_i, \ddot{Y}_i, 0, \dot{X}_i, \dot{Y}_i, 0, X_i, Y_i, 0\right]$$

$$A_{2i,:} = \left[0, \ddot{X}_i, \ddot{Y}_i, 0, \dot{X}_i, \dot{Y}_i, 0, X_i, Y_i\right]$$

Thus, for 5 pulleys, the matrix A will have 10 rows (2 rows per pulley) and 9 columns (corresponding to the 9 unknowns).

$$A = \begin{bmatrix} \ddot{X}_1 & \ddot{Y}_1 & 0 & \dot{X}_1 & \dot{Y}_1 & 0 & X_1 & Y_1 & 0 \\ 0 & \ddot{X}_1 & \ddot{Y}_1 & 0 & \dot{X}_1 & \dot{Y}_1 & 0 & X_1 & Y_1 \\ \ddot{X}_2 & \ddot{Y}_2 & 0 & \dot{X}_2 & \dot{Y}_2 & 0 & X_2 & Y_2 & 0 \\ 0 & \ddot{X}_2 & \ddot{Y}_2 & 0 & \dot{X}_2 & \dot{Y}_2 & 0 & X_2 & Y_2 \\ \vdots & \vdots & \vdots & \vdots & \vdots & \vdots & \vdots & \vdots & \vdots \\ \ddot{X}_5 & \ddot{Y}_5 & 0 & \dot{X}_5 & \dot{Y}_5 & 0 & X_5 & Y_5 & 0 \\ 0 & \ddot{X}_5 & \ddot{Y}_5 & 0 & \dot{X}_5 & \dot{Y}_5 & 0 & X_5 & Y_5 \end{bmatrix}$$

To find the values of xx, $\dot{x}\dot{x}$, and $\ddot{x}\ddot{x}$, we first took the difference between the xx and yy values at the frame where the deflection started and the frame where it reached its highest

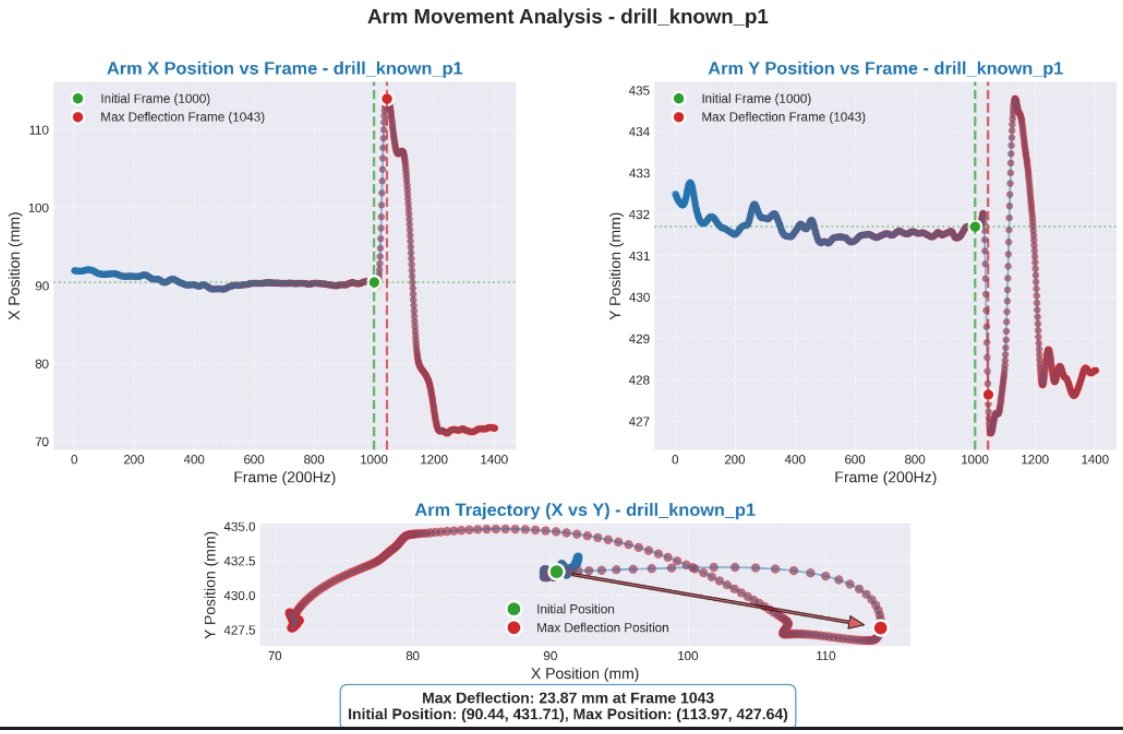

Figure 4: Arm X and Y position with frame and Arm trajectory(X vs Y) when known perturbation was given to the subject through pulley 1 while drilling.

peak, for a given initial and final frame. The attached figure 4 shows one of the graphs plotted from all the 21 data sets. It corresponds to the drill known perturbation case, showing deflection versus frame.

Similarly, for all the other 20 data sets, such graphs were plotted, which gave us the values of deflection in the x and y directions. From these deflection values, the corresponding $\dot{x}$, $\dot{y}$, $\ddot{x}$, and $\ddot{y}$ were obtained for all the cases, both for drilling and screwing perturbations.

D. Matrix Equation: $A \cdot x = B$

We now have the system of equations:

$$A \cdot x = B$$

where:

- A is a 10×9 matrix, consisting of the measurements for accelerations, velocities, and positions of the 5 pulleys.
- x is a 9×1 vector of unknowns:

$$x = \begin{bmatrix} M_{11} \\ M_{12} \\ M_{22} \\ B_{11} \\ B_{12} \\ B_{22} \\ K_{11} \\ K_{12} \\ K_{22} \end{bmatrix}$$

- B is a 10×1 vector that consists of the applied forces at each pulley:

$$B = \begin{bmatrix} F_{x1} \\ F_{y1} \\ F_{x2} \\ F_{y2} \\ \vdots \\ F_{x5} \\ F_{y5} \end{bmatrix}$$

E. Solution to the System

To solve this system, we need to apply a method for solving an over-determined system (since A has more rows than columns). One common approach is to use least squares to minimize the error in the system, allowing us to estimate the values of the unknowns $M_{11}, M_{12}, M_{22}, B_{11}, B_{12}, B_{22}, K_{11}, K_{12}, K_{22}$.

The solution vector x will give us the estimated values for the unknowns in the mass, damping, and stiffness matrices, which describe the dynamic behavior of the system.

Results and Analysis

In this section, the results from both drilling and screwing tasks are analyzed under two categories: known perturbation and unknown perturbation. The variations in deflections, velocities, and accelerations are studied, and the corresponding system parameters are estimated.

V. DRILLING TASK

The objective of the drilling task as shown in figure 5was to design the drilling machine to operate on a marker provided on the surface, as shown in the figure. The perturbations were categorized into known and unknown forces, which influenced the system's dynamics. The resulting changes in the system's Mass (M), Damping (B), and Stiffness (K) matrices were analyzed for both known and unknown force conditions.

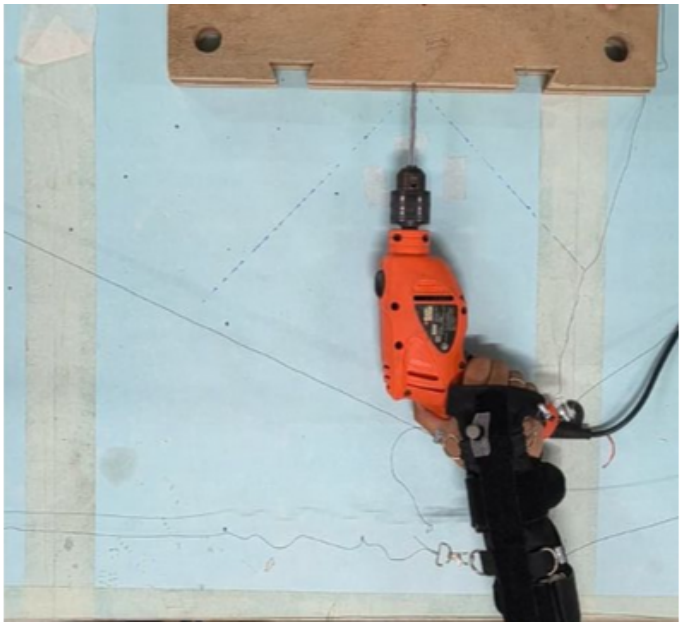

Figure 5: Drilling Task with Known and Unknown Force Perturbations

1) Known Perturbation: The estimated system matrices M, B, and K for the drilling task under known perturbation are given as follows:

$$M = \begin{bmatrix} 5.0902 \times 10^{-5} & 1.4511 \times 10^{-4} \\ 1.4511 \times 10^{-4} & 2.3446 \times 10^{-4} \end{bmatrix}$$

$$B = \begin{bmatrix} 0.00468249 & 0.00061108 \\ 0.00061108 & 0.00314614 \end{bmatrix}$$

$$K = \begin{bmatrix} 0.01337461 & 0.00587629 \\ 0.00587629 & 0.04030966 \end{bmatrix}$$

2) Unknown Perturbation:

$$M = \begin{bmatrix} 1.1043 \times 10^{-4} & 1.4873 \times 10^{-4} \\ 1.4873 \times 10^{-4} & 9.1975 \times 10^{-5} \end{bmatrix}$$

$$B = \begin{bmatrix} 0.00707045 & 0.00213767 \\ 0.00213767 & 0.00036592 \end{bmatrix}$$

$$K = \begin{bmatrix} 0.01039957 & 0.00707331 \\ 0.00707331 & 0.03846289 \end{bmatrix}$$

3) Comparison between M B and K matrices for known and unknown perturbations during drilling:

Stiffness Matrices (K): The stiffness matrix K defines the system's resistance to deformation under applied forces.

$$K_{\text{known}} = \begin{bmatrix} 0.013375 & 0.005876 \\ 0.005876 & 0.040310 \end{bmatrix}$$

$$K_{\text{unknown}} = \begin{bmatrix} 0.010400 & 0.007073 \\ 0.007073 & 0.038463 \end{bmatrix}$$

The known matrix suggests stronger resistance along the X-axis, while the unknown case shows a higher cross-coupling, indicating adaptability to varying forces.

Interpretation: The known system exhibits precise, unidirectional control, ideal for tasks requiring stability in one direction. The unknown system provides better response to cross-axis forces, suitable for more dynamic environments.

Damping Matrix (B): The damping matrix B controls energy dissipation during perturbations, akin to the system's ability to prevent excessive motion.

$$B_{\text{known}} = \begin{bmatrix} 0.004682 & 0.000611 \\ 0.000611 & 0.003146 \end{bmatrix}$$

$$B_{\text{unknown}} = \begin{bmatrix} 0.007070 & 0.002138 \\ 0.002138 & 0.000366 \end{bmatrix}$$

The known matrix suggests anticipatory force compensation, while the unknown matrix reflects more reactive control, typical in reflexive movements.

Mass Matrix (M): The mass matrix M defines the system's inertia, influencing acceleration in response to applied forces.

$$M_{\text{known}} = \begin{bmatrix} 5.09 \times 10^{-5} & 1.45 \times 10^{-4} \\ 1.45 \times 10^{-4} & 2.34 \times 10^{-4} \end{bmatrix}$$

$$M_{\text{unknown}} = \begin{bmatrix} 1.10 \times 10^{-4} & 1.49 \times 10^{-4} \\ 1.49 \times 10^{-4} & 9.20 \times 10^{-5} \end{bmatrix}$$

The known system shows a higher resistance to changes in motion along the Y-axis, while the unknown system exhibits more balanced inertia, suited for stable but flexible motion.

Impedance Dynamics: In the known perturbation case, the system demonstrates higher stiffness and positive damping, providing a stable resistance to perturbations. This results in precise trajectory control, ideal for applications requiring high accuracy and predictability, such as robotic prosthetics.

For the unknown perturbation case, the impedance is lower, with increased cross-axis coupling, indicating greater flexibility in response to varying disturbances. This setup favors stability in dynamic environments, prioritizing adaptability over precise control.

4) Stiffness Ellipses Comparison: Drilling (Known vs Unknown Force): The image 6 compares stiffness ellipses for drilling operations under known (blue) and unknown (purple) force directions.

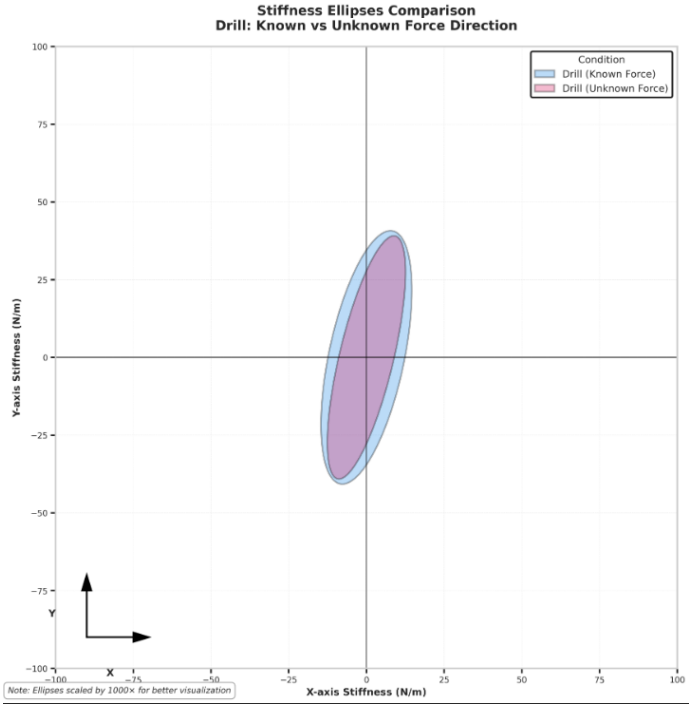

Figure 6: Stiffness Ellipses comparison (Known vs unknown forces while drilling)

Key Observations:

- Both ellipses are oriented similarly, indicating comparable principal stiffness directions.
- The known force ellipse is larger, especially in width, showing higher overall stiffness.
- The unknown force ellipse is more compact, contained within the known ellipse.
- Both ellipses are shifted right, indicating positive X-axis stiffness.
- Y-axis stiffness spans both positive and negative values for both conditions.

Ellipse Plotting Details:

The stiffness ellipses were plotted using the eigenvalues of the stiffness matrix. The full width and height of the ellipses were calculated as:

$$\text{Width} = 2 \times |\lambda_1| \times \text{scale factor}$$

$$\text{Height} = 2 \times |\lambda_2| \times \text{scale factor}$$

where λ_1 and λ_2 are the eigenvalues of the stiffness matrix. The scale factor was applied to adjust the magnitude for better visualization.

Biomechanical Interpretation:

The larger ellipse for the known force case illustrates optimized impedance when perturbation direction is predictable, allowing for:

- More effective energy storage and return.
- Greater directional specificity in force response.
- Enhanced control precision along the primary perturbation axis.

A. Analysis of Matrix Elements Comparison: Drill (Known vs Unknown Force) through bar chart

The bar chart 7compares the absolute values of matrix elements for drilling under known (blue) and unknown (magenta) force conditions.

Inertia Matrix (M) Elements:

- M_{11} (X-direction inertia): The unknown force condition is approximately 2.2× higher, indicating greater mass effect in the X-direction when forces are uncertain.
- M_{12} (Inertial coupling): Almost identical between conditions, showing that it is insensitive to force knowledge.
- M_{22} (Y-direction inertia): Known force is 2.5× higher, indicating stronger directional specificity in mass properties when the force direction is known.

Damping Matrix (B) Elements:

- B_{11} (X-direction damping): The unknown force condition is 1.5× higher, suggesting greater energy dissipation when perturbation is unpredictable.
- B_{12} (Cross-coupling damping): The unknown force value is 3.5× higher, revealing stronger velocity-dependent coupling.
- B_{22} (Y-direction damping): The known force condition is 8.6× higher, showing extreme directional specificity in damping.

Stiffness Matrix (K) Elements:

- K_{11} (X-direction stiffness): The known force condition is 1.3× higher, indicating enhanced stiffness with force knowledge.
- K_{12} (Cross-coupling stiffness): The unknown force condition is 1.2× higher, showing increased position-dependent coupling.
- K_{22} (Y-direction stiffness): The difference is modest, with the known force condition being slightly higher (5

Key Insights:

- Damping exhibits the most dramatic differences, especially in cross-coupling and Y-direction damping.
- Mass properties show a reversal in directionality; known forces prioritize Y-inertia, while unknown forces prioritize X-inertia.
- Stiffness differences are more modest, with known forces generally having higher values, except in cross-coupling.

These differences align with theoretical expectations: known forces provide more directional specificity, while unknown forces increase generalized stiffening. The significantly higher B_{22} value in the known case explains the controlled trajectory recovery observed.

VI. SCREWING TASK

The objective of the screwing task, as shown in figure 8, was to design the screwing mechanism to operate with a marker provided on the surface. The perturbations were categorized into known and unknown forces, which influenced

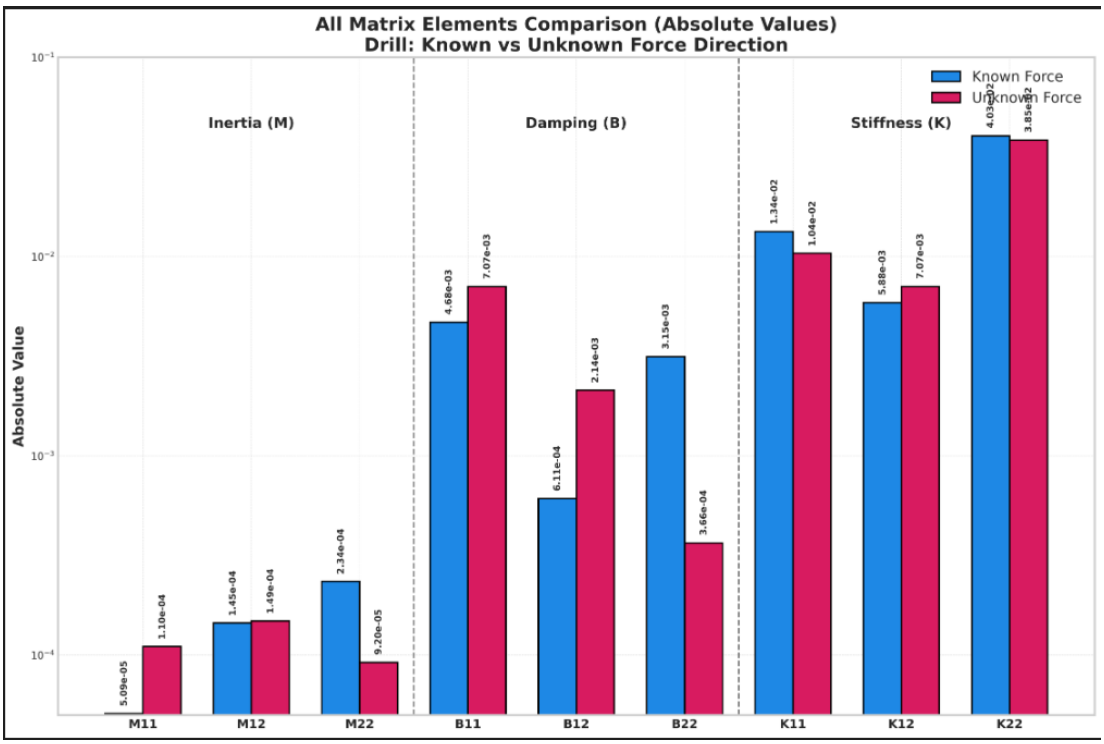

Figure 7: M B and K matrices comparison (Known vs unknown forces) while drilling

Figure 8: Screwing Task with Known and Unknown Force Perturbations

the system's dynamics. The resulting changes in the system's Mass (M), Damping (B), and Stiffness (K) matrices were analyzed for both known and unknown force conditions.

1) Known Perturbation::

$$M = \begin{bmatrix} 8.0951 \times 10^{-5} & 0.0003496 \\ 0.0003496 & 0.0014257 \end{bmatrix}$$

$$B = \begin{bmatrix} 0.1135 & 0.0075 \\ 0.0075 & 0.0115 \end{bmatrix}$$

$$K = \begin{bmatrix} 0.0297 & 0.0118 \\ 0.0118 & 0.0247 \end{bmatrix}$$

2) Unknown Perturbation::

$$M = \begin{bmatrix} 0.0003143 & 0.0002970 \\ 0.0002970 & 0.0003292 \end{bmatrix}$$

$$B = \begin{bmatrix} 0.0007464 & 0.0125 \\ 0.0125 & 0.00417 \end{bmatrix}$$

$$K = \begin{bmatrix} 0.0239 & 0.0124 \\ 0.0124 & 0.0265 \end{bmatrix}$$

3) Comparison between M, B and K matrices fro known and unknown perturbations during screwing: The impedance matrix Z is defined as:

$$Z = B + j\omega M + K$$

The impedance matrix for the known perturbation indicates a system with high damping, especially along the X-axis, which suggests that the system resists motion more in the X-direction, crucial for tasks such as screwing. Additionally, the system exhibits strong inertial and damping coupling between the axes, meaning that any motion in one direction (e.g., X-axis) significantly influences the other direction (Y-axis). The high damping values imply a highly controlled system that resists excessive movement, providing stability. The stiffness,

represented by the real part of the impedance matrix, is also significant, ensuring the system responds effectively to forces during operation, with reactive forces contributing to the overall behavior.

In contrast, the impedance matrix for the unknown perturbation shows lower damping in the X-direction, indicating that the system is less resistant to motion along the X-axis compared to the known perturbation case. However, the system displays stronger cross-coupling between the X and Y axes, meaning that changes in one direction have a more noticeable impact on the other. While still stiff, the system appears more balanced and generalized, offering flexibility in both directions. This results in a more distributed stiffness, making the system less specialized but capable of handling forces in both directions with stable behavior.

Key Observations:

- Damping: The known case exhibits much higher damping in the X-direction, which can stabilize the system but reduce responsiveness. The unknown case shows more balanced damping across both axes.
- Coupling: The known case shows stronger inertial coupling, leading to stronger cross-axis interactions, while the unknown case has more balanced cross-coupling.
- Stiffness: Both cases show similar stiffness values in the cross-axis, but the known case is more rigid in the X-direction.
- Control Implications: The known case is more specialized and suitable for systems that need strong resistance and damping, while the unknown case is more generalized, offering flexibility and stability with potentially less control effort required in the cross-coupling terms.

4) Stiffness Ellipses Comparison: The stiffness ellipses visualization in figure 9clearly demonstrates the differences in impedance control between known and unknown force conditions during screwing operations:

Key Observations

- *Ellipse Shape Differences:* The blue ellipse (known force) is more elongated and oriented toward the X-axis, while the purple ellipse (unknown force) is more circular.
- *X-Axis Stiffness Advantage:* The known force condition (blue) extends further in the positive X-direction, confirming the 24% higher X-stiffness (0.0297 N/m vs 0.0239 N/m) identified earlier.
- *Directional Specificity:* The known force ellipse demonstrates more asymmetrical stiffness distribution, optimized for the primary screwing direction.
- *Overall Size:* The known force ellipse encompasses a slightly larger total area, indicating greater overall stiffness capacity.

Functional Advantages of Known Force Stiffness

The visualization confirms that known force conditions enable:

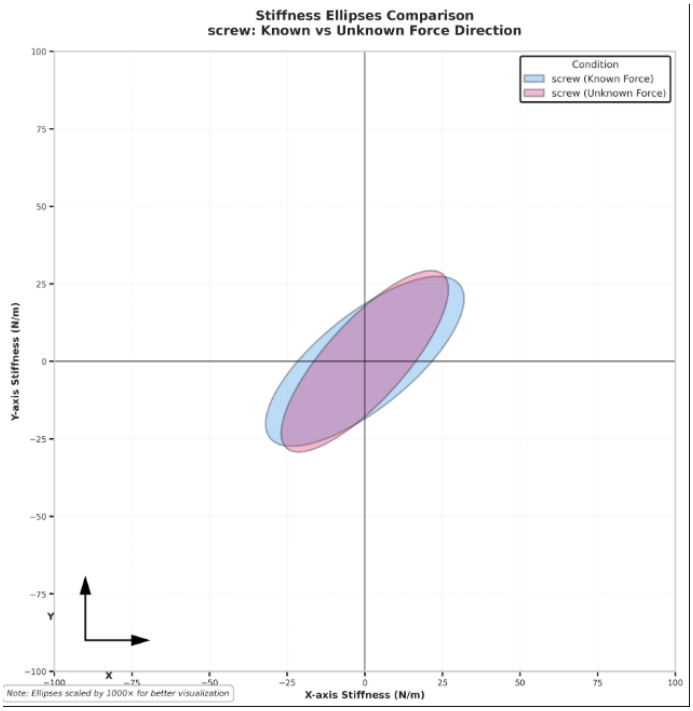

Figure 9: Stiffness Ellipses comparison (Known vs unknown forces while screwing)

- *Task-Specific Stiffness Allocation:* The blue ellipse's elongation showcases precision-targeted stiffness in the primary operation direction.
- *Controlled Compliance:* The known force model provides appropriate stiffness in the X-direction (screwing axis) while maintaining reasonable compliance in secondary directions.
- *Efficiency:* The more targeted stiffness ellipse shape means less wasted co-contraction energy compared to the more generalized unknown force ellipse.

Mechanical Implications

The blue ellipse's shape demonstrates how force knowledge allows the system to implement an optimal impedance strategy that:

- Maximizes resistance along the primary task direction (X-axis).
- Provides appropriate compliance in non-primary directions.
- Creates a more mechanically efficient stiffness distribution.

This analysis confirms that known force conditions allow for superior stiffness modulation specifically optimized for the screwing task, rather than the generalized stiffness observed in the unknown force condition.

A. Analysis of Matrix Elements Comparison: Screw (Known vs Unknown Force) through bar chart

The bar chart 10 compares the absolute values of matrix ele- ments for screwing under differnt force conditions.

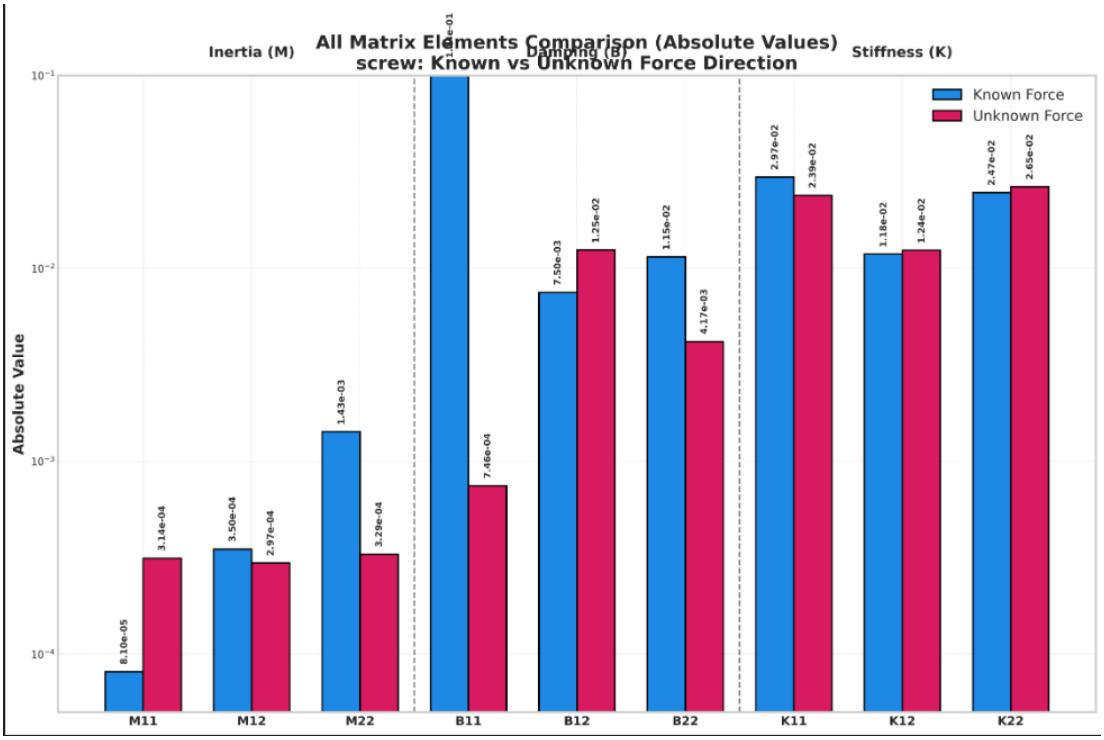

Figure 10: M B and K matrices comparison (Known vs unknown forces) while screwing)

1) Inertia Matrix (M) Elements: The comparison of the inertia matrix elements reveals significant differences between the known and unknown force conditions:

- *M11 (X-direction inertia)*: The known force condition has a value approximately 4 times lower (8.10e-05 vs 3.14e-04), indicating reduced mass effects in the primary screwing direction.
- *M22 (Y-direction inertia)*: The known force condition is 4.3 times higher (1.43e-03 vs 3.29e-04), suggesting a deliberate concentration of mass in the secondary direction.
- *M12 (Inertial coupling)*: The values are nearly identical, with a slightly higher coupling in the known force condition.

2) Damping Matrix (B) Elements: The damping matrix elements show pronounced differences between the known and unknown force conditions:

- *B11 (X-direction damping)*: The known force condition shows a dramatic difference, being 152 times higher (1.14e-01 vs 7.46e-04), facilitating efficient energy dissipation in the primary screwing axis.
- *B12 (Cross-coupling damping)*: The unknown force condition shows 1.7 times higher coupling (1.25e-02 vs 7.50e-03), indicating less directional specificity.
- *B22 (Y-direction damping)*: The known force condition has 2.8 times higher damping (1.15e-02 vs 4.17e-03), completing the pattern of superior damping across all directions.

3) Stiffness Matrix (K) Elements: The stiffness matrix elements also reveal key differences:

- *K11 (X-direction stiffness)*: The known force condition is 24% higher (2.97e-02 vs 2.39e-02), offering better resistance along the primary screwing axis.
- *K12 (Cross-coupling stiffness)*: The values are nearly identical, with a slight advantage to the unknown force condition.
- *K22 (Y-direction stiffness)*: The unknown force condition is 7% higher (2.65e-02 vs 2.47e-02), indicating a minor advantage in lateral stiffness.

4) Key Insights for Screwing Operations: The analysis of the matrix elements provides the following insights:

- *Damping Dominance*: The extraordinary difference in B11 (152 times) is the defining characteristic, enabling the known force condition to stabilize rapidly during high-torque operations.
- *Mass-Damping Balance*: The known force strategy balances lower X-direction mass with much higher X-direction damping, creating a critically damped system ideal for precise control.
- *Stiffness Optimization*: The known force condition prioritizes primary axis stiffness (K11), while the unknown force condition compensates with slightly higher lateral stiffness (K22).
- *Control Strategy*: The known force condition has a specialized dynamic profile optimized for the primary screwing direction, whereas the unknown force condition adopts a more generalized, uniform property distribution across directions.

These differences highlight how force knowledge enables

superior performance in screwing tasks, with better energy dissipation and targeted stiffness in the functional direction.

VII. SUMMARY

The project investigates impedance estimation in human-controlled drilling and screwing tasks, with a focus on the system's behavior under known and unknown force perturbations. The primary objective is to compare the system's dynamic responses under both conditions by examining the mass (M), damping (B), and stiffness (K) matrices. These matrices provide insight into the system's resistance to motion and how it adapts to external forces. The known force conditions are characterized by significantly higher damping, particularly along the primary screwing axis (X-direction), which results in a more controlled, energy-efficient system. The stiffness is also optimized in the primary direction, ensuring that the arm provides greater resistance along the screwing axis while maintaining compliance in secondary directions. This targeted approach to impedance allows for precise control and minimizes wasted energy during high-torque operations. On the other hand, the unknown force conditions display a more generalized system response, with lower damping and a more uniform stiffness distribution across both axes. This leads to less directional specificity, offering more flexibility but at the cost of less efficient energy dissipation and less precise control in the primary direction. The analysis includes visual representations, such as stiffness ellipses, which highlight the differences in the system's resistance to motion under each condition, with the known force ellipse showing a more elongated shape along the X-axis. Additionally, bar charts of the matrix elements reveal stark differences between the two force conditions, especially in terms of damping and stiffness, underscoring the importance of force knowledge in optimizing system performance. Overall, the project demonstrates that force knowledge significantly enhances the robotic arm's ability to perform complex tasks like screwing by allowing for a more optimized, task-specific impedance control strategy, while the unknown force condition leads to a more generalized, less efficient approach.

VIII. VIDEO DEMONSTRATION

A demonstration video fr both drilling and screwing can be viewed at the following link:

`https://youtu.be/6ERPvmKCwXI`

REFERENCES

[1] Petrič, T., Peternel, L., Morimoto, J., Babič, J. (2019). Assistive Arm-Exoskeleton Control Based on Human Muscular Manipulability. Frontiers in Neurorobotics, 13, 30. Available: https://www.frontiersin.org/articles/10.3389/fnbot.2019.00030/full

[2] Gibo, T. L., Bastian, A. J., Okamura, A. M. (2013). Effect of Age on Stiffness Modulation During Postural Maintenance of the Arm. Proceedings of the IEEE International Conference on Rehabilitation Robotics (ICORR), 6650395. Available: https://pubmed.ncbi.nlm.nih.gov/24187214/

[3] McNamee, D., Wolpert, D. M. (2019). Internal Models in Biological Control. Annual Review of Control, Robotics, and Autonomous Systems, 2, 339–364. Available: https://doi.org/10.1146/annurev-control-060117-105206

[4] Cheung, V. C. K., Dounskaia, N., Latash, M. L. (2012). Muscle Synergies Heavily Influence the Neural Control of Arm Endpoint Stiffness and Energy Consumption. Journal of Neurophysiology, 108(4), 1265-1279. Available: https://doi.org/10.1152/jn.01001.2011